Average and Detailed Modeling Approaches Emphasizing Subsystems in a Hybrid Mobile Refrigeration

Yue Cao, *Student Member*, *IEEE*, Philip T. Krein, *Fellow, IEEE*

Abstract—**Averaging-based and detailed dynamic models of hybrid electric power systems are presented, with emphasis on electric machines and drives. The objective is to compare technical and practical aspects associated with hybridization of refrigeration units in delivery trucks. Challenges unique to this hybrid application, including the thermal system interface and drive-cycle response, are introduced. The system topology is presented, and modeling approaches for each major subsystem, including an ac machine, the battery set, and converters, are discussed. An average modeling technique is fast enough to allow system-level power and efficiency to be evaluated over a long time interval. Compared to the average model, a detailed model including transient response and harmonics gives more accurate power loss estimates at the cost of slower simulation speed. The two models, interfaced with the thermal system, are examined with simulation studies in MATLAB/Simulink, showing the features of each model. Experimental setup and results are presented to validate the models.**

Index Terms—**Mobile refrigeration unit (MRU), hybrid power systems, electric drives, average model, dynamic models**

I. INTRODUCTION

Produce delivery trucks that require diesel-powered mobile refrigeration units (MRU) to maintain food freshness, like that in Fig. 1, consume significant energy [1-3]. The main engine may need to idle indefinitely when the truck is stopped for a delivery, or a separate small diesel engine may be dedicated to the refrigeration unit. It is becoming more necessary to comply with new laws and increasing customer demands for more environmentally friendly and fuel-efficient delivery vehicles [4]. This paper presents system-level models based on fast simulation that seeks to integrate electric drive and other subsystems for hybridization of MRUs based in part on the developments in [5]. Models based on averaging and based on more detailed dynamics are provided. The treatment focuses on electric machine dynamics including torque and speed responses to various delivery cycles and thermal loadings. The dynamic model includes switching voltage and current waveforms. It serves a validation check for average model accuracy and provides guidelines for hardware design.

Figure 1. A typical produce delivery truck with MRU
Source: FormerWMDriver on flickr.com

II. HYBRID POWER SYSTEM FOR MRU

A high-level system configuration of a proposed hybrid MRU is depicted in Fig. 2. In contrast to a more conventional system with dedicated small engine, this version takes in power from the main truck engine via an ac generator, and also has the option to connect to the grid. After power conversion and control, several electric motors drive compressors, fans, and blowers, comprising the thermal system. Heaters are needed to cover a full range of climate conditions, since an MRU is not specialized: the same truck might deliver fruit one day and frozen meat the next.

Fig. 3 shows the hybrid power system: the main engine shaft drives an ac generator, feeding an active rectifier that stabilizes its output dc bus, then an inverter operates an ac induction machine to drive the compressor; the battery connects at the dc bus, possibly through a separate dc-dc converter. Additional small motors to run fans and blowers are not shown. The differences between mobile and stationary refrigeration units include 1) frequent and drastic temperature changes due to loading and unloading of products, 2) a wide variety of truck operating profiles and environments depending on road conditions, delivery schedules, and outdoor temperatures, and 3) lack of access to consistent and reliable power sources.
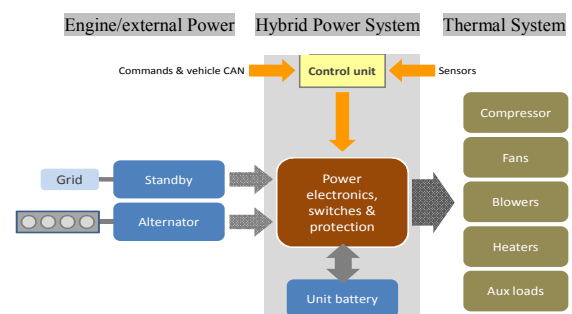
Figure 2. System configuration of the proposed MRU
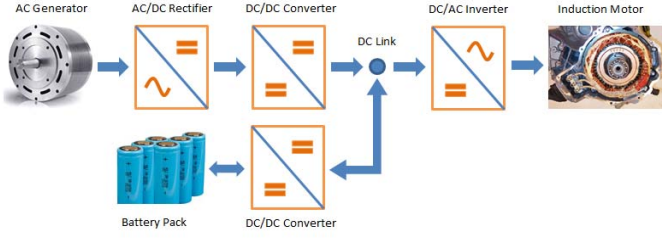
Figure 3. Hybrid power system structure in the simulation model

III. AVERAGE MODELING APPROACH

The average modeling approach seeks to model energy flows and power balances, including power losses in each subsystem (motor, converter, battery, etc.). Conduction and switching devices losses are modeled based on in equivalent steady state conditions. Most losses have a direct relationship with the associated currents. Calculated output currents from one subsystem are passed as input currents to the next subsystem. Energy flows can be examined in either direction, with input and output currents changing roles. Machine mechanical losses must also be included. These can be inferred from machine data sheets and basic tests.

Since the ac generator is coupled to the drive engine, its operating speed is linked to a dynamic vehicle drive cycle, and ranges from 1750 to 5000 RPM. MRUs experience more complicated operating sequences than automobiles, so conventional drive cycles have limited value. For simulation studies reported here, drive cycle data were obtained from an industry study that recorded typical truck driving conditions [6]. The ac generator is modeled as a 3-phase permanent magnet synchronous machine (PMSM) with continuous output rating of 17.3 kW. The ac motor that drives the compressor is modeled as a 3-phase 12 HP 460 V 60 Hz induction machine (IM). The IM and PMSM models employ conventional per-phase steady-state equivalent circuits [7].

The rectifier, inverter, and any dc-dc converters are power electronic elements with switching loss and conduction losses in the IGBTs. These can be estimated as [8]

$$P_{cond} = \frac{2\sqrt{2}I_{rms}V_{on}}{\pi} + I_{rms}^2 R_{ds} \quad (1)$$

and

$$P_{switch} = \frac{2\sqrt{2}I_{rms}V_{bus}}{\pi} f_{switch} \frac{t_{on}+t_{off}}{2} \quad (2)$$

The conduction loss can be modeled by means of an ideal switch in series with a forward voltage drop (V_{on}) and a series resistor (R_{ds}). In the switching loss calculation, f_{switch} is the inverter switching frequency. Times t_{on} and t_{off} are the IGBT switching rise and fall delay times, respectively, which are found in device datasheets. V_{bus} is the main dc bus voltage.

The battery model is based on the circuit in Fig. 4, in which voltage source, resistors and capacitors depend nonlinearly on the battery's state of charge (SOC)

$$\ln(V,C,R) = a_0 + a_1 \ln(SOC) + ... + a_6 \ln^6(SOC) = \sum_{k=0}^{6} a_k \ln^k(SOC) \quad (3)$$

SOC is modeled as in [5] as

$$SOC(t) = SOC_{initial} + \int_0^t f_1[i_{charge}(t)] \times i_{charge}(t)dt + \int_0^t f_2[i_{discharge}(t)] \times i_{discharge}(t)dt \quad (4)$$

Functions f_1 and f_2 are look-up tables from current testing [9]. The coefficients in (4) found in [5] are from curve fitting of experimental data of V, C, and R versus SOC. Single-cell data (current, SOC) were extracted from measurements of the Panasonic CGR18650A 3.7 V, 2.2 A-h Li-ion batteries [10]. The battery terminal voltage is then calculated as

$$V_t = V_{oc} - I_c (R_{series} + R_{ts} \| \frac{1}{sC_{ts}} + R_{tm} \| \frac{1}{sC_{tm}} + R_{th} \| \frac{1}{sC_{th}}) \quad (5)$$
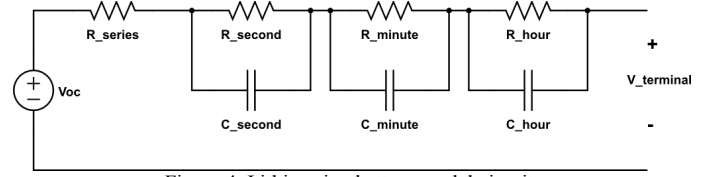
Figure 4. Lithium-ion battery model circuit

Notice that the model includes explicit dynamics on time scales of seconds, minutes, and hours.

IV. DETAILED MODELING APPROACH

A detailed dynamic model was constructed in Simulink/SimPowerSystems. This modeling approach differs from the average model in several areas. The converter semiconductor devices are treated as switches with parasitic losses. The electric machines (PMSM, IM) are modeled as differential equations

$$V_{qs} = R_s i_{qs} + d\varphi_{qs}/dt + \omega\varphi_{qs}$$
$$V_{ds} = R_s i_{ds} + d\varphi_{ds}/dt + \omega\varphi_{ds}$$
$$V'_{qr} = R'_r i'_{qr} + d\varphi'_{qr}/dt + (\omega-\omega_r)\varphi'_{dr}$$
$$V'_{dr} = R'_r i'_{dr} + d\varphi'_{dr}/dt + (\omega-\omega_r)\varphi'_{qr} \quad (6)$$
$$T_e = 1.5p(\varphi_{ds}i_{qs} - \varphi_{qs}i_{ds})$$
$$d\omega_m/dt = (1/2H)(T_e - F\omega_m - T_m)$$

that produce transient waveforms [11]. Filters are also included between components. The dc-dc converter is feedback controlled to stabilize the dc bus voltage.

A scalar volts-per-hertz (V/f) control (Fig. 5) is implemented in the IM drive (Fig. 6). The IM and PMSM are controlled to respond robustly to a wide range of torque and speed commands from the thermal system, and to engine dynamics associated with the vehicle driving cycle.
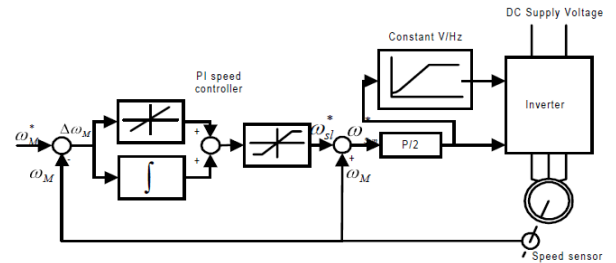
Figure 5. IM V/f closed-loop control diagram
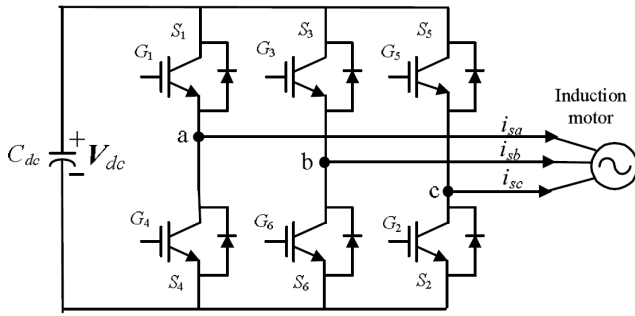
Figure 6. dc-ac inverter circuit tied to the ac motor

V. SIMULATION STUDY

A comprehensive simulation must be run for the integrated thermal-electrical system. It is important to evaluate each subsystem's performance under real-life scenarios. The scenario includes the vehicle drive cycle, dynamic thermal loading demand based on the desired truck container temperature and ambient temperature, door open and close events, connection to "shore" power, etc. The energy flow is developed in reverse order: based on thermal requirements, the compressor has known speed and torque requirements. These in turn are supplied by the induction machine, and to this machine by the inverter. The inverter draws power from the generator or the batteries. Generator operation is linked to engine RPM during the vehicle drive cycle, sitting idle at minimum speed when the vehicle stops.

For a complete study, simulation is to analyze a delivery cycle lasting eight hours or more. System-level simulation must be faster than real time to make this useful. The average model tolerates a wide range of sampling times up to 0.1 s to accommodate different thermal or other electrical interfacing requirements. The detailed model has a maximum sampling time of 5 μs. The average model takes three minutes to simulate one hour of a delivery run, while the detailed model operates only slightly faster than real time and is not as useful for for-cycle studies.

To demonstrate the capabilities of the average model, a system simulation from 20,000 s to 29,000 s, corresponding to 1:00 PM to 3:30 PM during a typical day's delivery schedule, was prepared. The motor operates when there is demand from the thermal system. The battery is charged, if below a preset SOC value, when the generator runs, and it is discharged when the motor is on while the truck is not moving. Figs. 7-9 show the power levels at each component in the hybrid power system. Notice that the time units reflect an interval nearly three hours long.
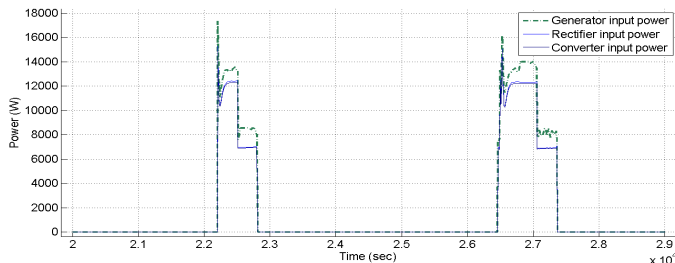
Figure 7. Power levels at the generator, rectifier, and converter
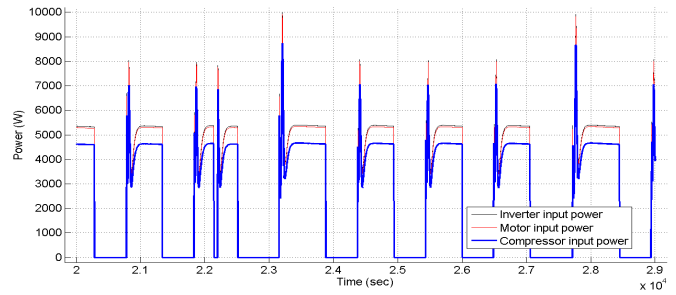
Figure 8. Power levels at the inverter, motor, and compressor
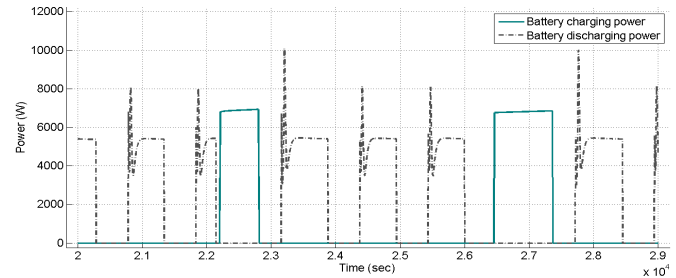
Figure 9. Battery charging and discharging power

From the detailed model, Fig. 10 shows dynamic response of rotor speed, stator current, and electromagnetic torque of the IM during a compressor start. The simulation starts at system time 5400 s, and the interval shown is less than 1.5 s. Note that it takes about 0.5 s for the rotor to ramp up to the desired speed, 1720 RPM. After another 0.5 s, a speed of 1780 RPM is commanded, and further transient response is observed. Fig. 11 shows that the dc bus voltage is held to 700 V throughout the run, reflecting the capabilities of an active rectifier and a dc-dc converter to interface the batteries. The inverter PWM modulation index is ramped up gradually to the desired value in this V/f strategy. Details of the high-frequency switching IM stator voltage can be observed.
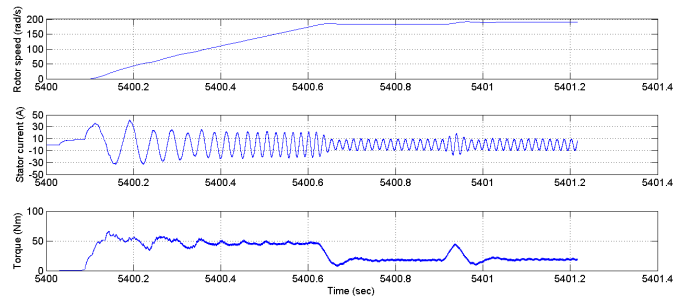
Figure 10. IM rotor speed, stator current, and torque during transient
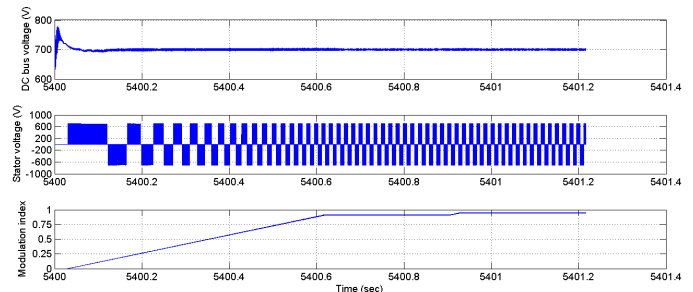
Figure 11. Inverter dc bus voltage, output voltage, and modulation index

1134

Similarly detailed waveforms on the PMSM side can be obtained. Fig. 12 shows the generated voltage and current during the same time interval, and Fig. 13 illustrates the output torque and speed from the generator. The speed is tied to the truck drive cycle. In addition, Fourier spectra of the IM and PMSM stator currents are analyzed in Fig. 14.
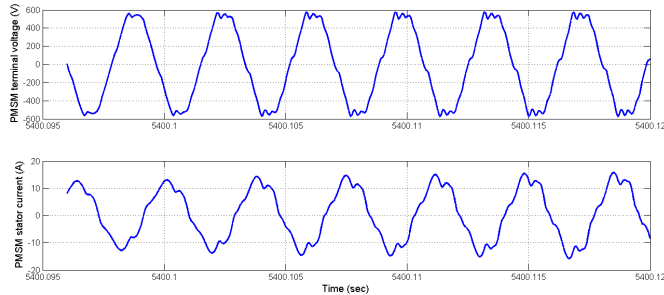
Figure 12. PMSM terminal voltage and stator current

The detailed model also serves as a check for the average model. Fig. 15 plots ten efficiency values on the engine power supply efficiency curve, and Table 1 lists the detailed data for these ten points. The two efficiency curves are within 5% of each other. Generally, the detailed model efficiency is somewhat lower since it is more refined.
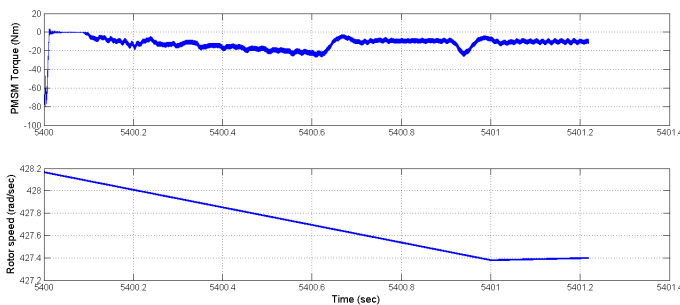
Figure 13. PMSM generated torque and rotor speed
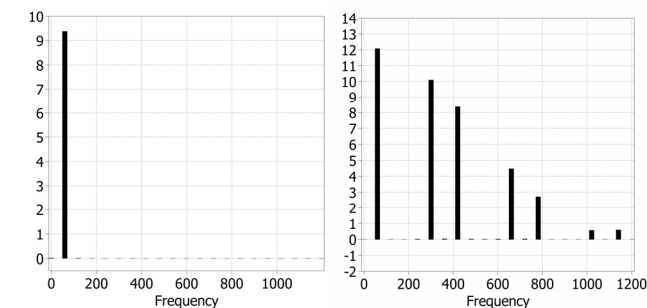
Figure 14. Fourier spectra for IM current (left) and PMSM current (right)
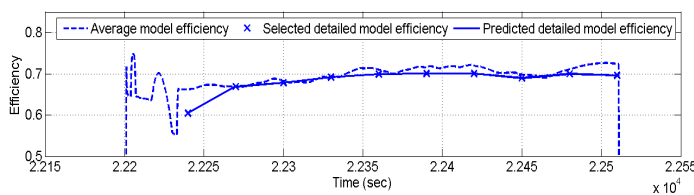
Figure 15. Simulated efficiency comparison for average and detailed models

Table 1. Simulated power and efficiency data for the detailed model

Generator RPM	Motor RPM	Torque (Nm)	Input Power (W)	Output Power (W)	Efficiency
2909	1786	15.31	5132	3099	0.603
4056	1782	19.56	5818	3891	0.668
4233	1779	22.76	6604	4479	0.678
4227	1778	24.11	6936	4797	0.691
3899	1777	24.62	6890	4818	0.699
3689	1777	24.78	6918	4849	0.700
3571	1777	24.82	6932	4858	0.700
4188	1777	24.83	7048	4860	0.689
3863	1777	24.82	6934	4855	0.700
3347	1777	24.8	6970	4850	0.695

VI. EXPERIMENTAL VALIDATION

Tests of the generator and the ac-dc rectifier were conducted separately [12]. A three-phase PMSM, the one modeled in Simulink, was used in the experimental tests. This device was used previously for an electric air conditioning unit in a city bus. Different loads were applied for each of various speed settings, and the corresponding powers and efficiencies were obtained through direct measurement, as shown in Fig. 16.
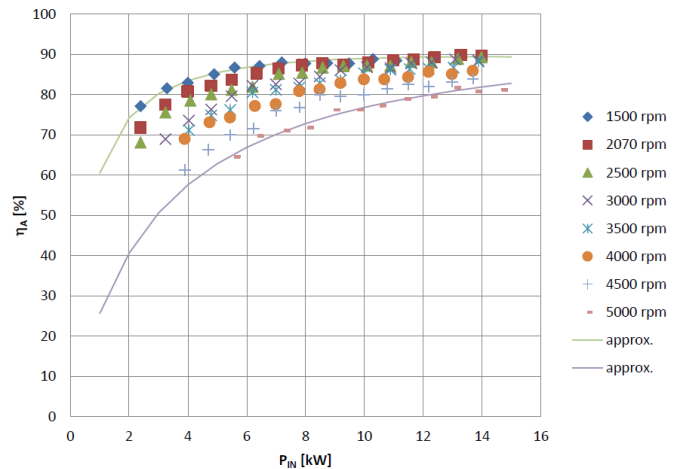
Figure 16. PMSM efficiency versus power at different speeds, from [12] courtesy of Thermo King Corporation, used by permission.

A hardware test bed for the variable frequency ac motor drive, including the dc-ac inverter and the motor is shown in Fig. 17. The system operates at about 1/6 scale compared to the vehicle system. A three-phase 230 V 2 HP 4-pole IM was chosen, and a modular dc-ac inverter was used. The control box of the inverter is based on a TI-2812 DSP and commanded by MATLAB/Simulink [13]. The torque and speed profiles were referenced from the thermal system demand. The measured efficiency was on average about 5% lower than the simulated efficiency, as shown in Fig. 18. This

is expected since the test machine used for this experiment has a rated efficiency about 5% lower than the simulated machine. Figs. 19 and 20 show the IM rotor speed and stator phase current during the initial one second of start-up.
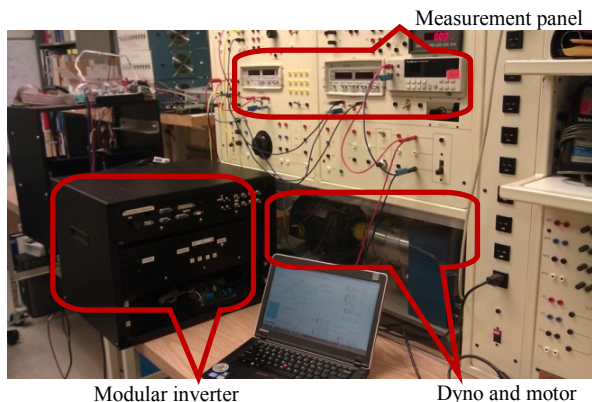
Figure 17. Experiment setup for the power system testing.
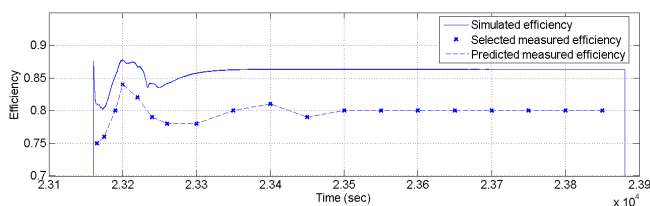
Figure 18. Measured efficiency compared to simulated efficiency
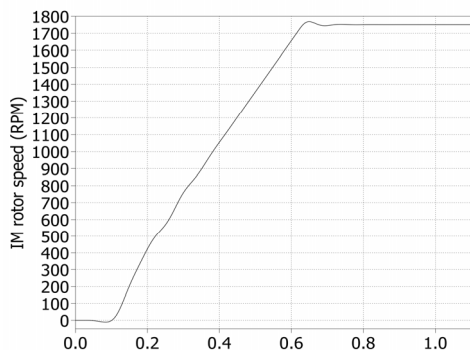
Figure 19. Measured IM rotor speed during transient
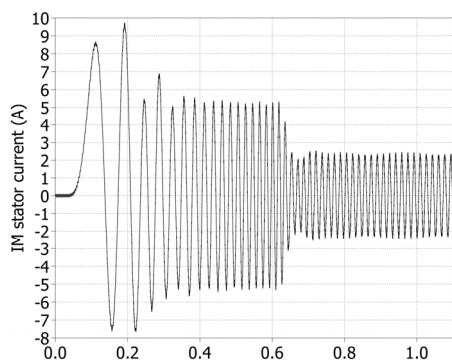
Figure 20. Measured IM stator current during transient

VII. CONCLUSION

A hybrid power system for mobile refrigeration has been modeled using an average approach and a detailed approach. The model has been validated through successful simulation and experimental work. With the average model, a complete thermal-electric system simulation has been built and serves as a basis for future hybrid system optimization studies. The complete simulation operates about twenty times faster than real time. The detailed model can be used for hardware design, and it has the development potential in a few directions, including 1) advanced existing or novel motor drive control techniques for highly efficient and precise internal loading requirement, and 2) multilevel converter based motor drive for improving efficiency and reducing motor stress, especially under high power requirements. It runs slightly faster than real time, but its complexity and fast sampling times make it less suited for integration with thermal subsystems.

REFERENCES

[1] T. van Keulen, et al., "Design, implementation, and experimental validation of optimal power split control for hybrid electric trucks," *Control Engineering Practice*, vol. 20, no. 5, pp. 547-558, May 2012.

[2] T. Hofman, et al., "Hybrid component specification optimization for a medium-duty hybrid electric truck," *International Journal of Heavy Vehicle Systems*, vol. 15, no. 2-4, pp. 356-392, 2008.

[3] L. He, et al., "Impact of vehicle usage on consumer choice of hybrid electric vehicles," *Transportation Research Part D: Transport and Environment*, vol. 17, no. 3, pp. 208-214, May 2012.

[4] C. V. Kulkarni, "Modeling and the performance analysis of transportation refrigeration units with alternate power systems," Ph.D. dissertation, Mechanical and Aeronautical Engineering, Univ. of California, Davis, CA, 2007.

[5] Y. Cao and P. T. Krein, "An average modeling approach for mobile refrigeration hybrid power systems with improved battery simulation," to appear in *Proc. IEEE Transportation Electrification Conf.*, June 2013.

[6] R. A. Jackey, "A simple, effective lead-acid battery modeling process for electrical system component selection," The Mathworks Inc., Novi, MI, Rep. 2007-01-0778, 2007.

[7] A. E. Fitzgerald, C. Kingsley, and S. D. Umans, *Electric Machinery*, 6th ed. NY: McGraw Hill, 2003, pp. 306-348.

[8] P. T. Krein, *Elements of Power Electronics*. New York: Oxford University Press, 1998, pp. 451-530.

[9] R. C. Kroeze and P. T. Krein, "Electrical battery model for use in dynamic electric vehicle simulations," in *Proc. IEEE Power Electronics Specialists Conf.*, 2008, pp. 1336-1342.

[10] R. C. Kroeze, "Electrical battery model for use in dynamic electric vehicle simulations," M.S. thesis, Electrical and Computer Engineering, Univ. of Illinois, Urbana, IL, 2008.

[11] P. C. Krause, O. Wasynczuk, and S. D. Sudhoff, *Analysis of Electric Machinery and Drive Systems*, 2nd ed. Edison, NJ: Wiley-IEEE Press, 2002, pp. 525-556.

[12] P. Kadanik, et al., "Transport hybridization study sponsor update – Thermo King and Ingersoll Rand," unpublished, 2012.

[13] J. Kimball, et al., "Modular inverter for advanced control applications," Grainger Center for Electric Machinery and Electromechanics, Urbana, IL, CEME-TR-2006-01, 2006.